Journal of Magnetic Resonance 213 (2011) 14–21

Contents lists available at ScienceDirect

Journal of Magnetic Resonance

journal homepage: www.elsevier.com/locate/jmr

# Band-selective chemical exchange saturation transfer imaging with hyperpolarized xenon-based molecular sensors

Tyler Meldrum [a,c], Vikram S. Bajaj [a,c,*], David E. Wemmer [b,c], Alexander Pines [a,c]

[a] Materials Sciences Division, Lawrence Berkeley National Laboratory, Berkeley, CA 94720, USA
[b] Physical Biosciences Division, Lawrence Berkeley National Laboratory, Berkeley, CA 94720, USA
[c] Department of Chemistry, University of California, Berkeley, CA 94720, USA

ARTICLE INFO

*Article history:*
Received 27 June 2011
Available online 13 July 2011

*Keywords:*
MRI
Contrast agent
Chemical exchange saturation transfer
Xenon
Hyperpolarization

ABSTRACT

Molecular imaging based on saturation transfer in exchanging systems is a tool for amplified and chemically specific magnetic resonance imaging. Xenon-based molecular sensors are a promising category of molecular imaging agents in which chemical exchange of dissolved xenon between its bulk and agent-bound phases has been use to achieve sub-picomolar detection sensitivity. Control over the saturation transfer dynamics, particularly when multiple exchanging resonances are present in the spectra, requires saturation fields of limited bandwidth and is generally accomplished by continuous wave irradiation. We demonstrate instead how band-selective saturation sequences based on multiple pulse inversion elements can yield saturation bandwidth tuneable over a wide range, while depositing less RF power in the sample. We show how these sequences can be used in imaging experiments that require spatial–spectral and multispectral saturation. The results should be applicable to all CEST experiments and, in particular, will provide the spectroscopic control required for applications of arrays of xenon chemical sensors in microfluidic chemical analysis devices.



## 1. Introduction

Molecular imaging promises minimally invasive and anatomically specific localization of chemical phenomena in morphologically detailed magnetic resonance images. This presents obvious applications to early detection of pathological states in living organisms, but can also be applied to chemical and biochemical profiling of complex mixtures [1]. Molecular imaging contrast agents for both applications are commonly molecular or supramolecular assemblies that couple a contrast center, which perturbs a magnetic resonance observable, to a recognition or targeting moiety. Many contrast agents operate by affecting the relaxation properties of exchanging water, a concentrated solvent. The effect on relaxation can take place either passively, in which case the contrast agents are simply targeted to interesting sites, or be switched on upon binding to a dilute analyte. A recent innovation involves the use of paramagnetic lanthanides to generate a distinct resonance corresponding to the bound pool of the exchanging water, bringing the chemical exchange saturation transfer contrast mechanism under spectroscopic control [2]. Operating on similar principles, xenon-based molecular sensors are targeted, xenon-binding, host–guest complexes that reversibly bind xenon, generating a spectrally distinct species that can perturb the signal of hyperpolarized xenon gas dissolved in a bulk aqueous phase [3].

According to these principles, the ideal magnetic resonance contrast agent should operate like a transistor, amplifying a small signal (the analyte) in a controlled and linear way by proportionally perturbing a larger signal (the solvent or other abundant medium) over a wide dynamic range. Xenon-based molecular sensors fulfill these requirements, due primarily to several favorable properties of xenon itself. First, xenon has a very large chemical shift range due to the high polarizability of its electrons [4]. Consequently, one can selectively perturb either the population of xenon in bulk solvent or that encapsulated by a host sensor molecule [3,5] with high specificity [6]. Further, in most cases, xenon exchanges rapidly between the cage-bound and free forms, making sensitivity enhancements by chemical exchange saturation transfer (CEST, [7–10]) possible [11,12]. Because the chemical shift range of xenon is large, many targeted analytes can be distinguished by frequency changes resulting from minor chemical alterations to the host molecule [13,14]. Finally, xenon is hyperpolarizable by spin-exchange optical pumping [15], is chemically and biologically inert, and is water soluble. Recently, we have demonstrated that sub-picomolar concentrations of a novel xenon sensor construct can be detected within 20 s of saturation transfer [16].

In the above examples, the xenon chemical sensor contains the cage-like molecule cryptophane, a member of a class of small, organic structures that act as a host for xenon [17]. The conjugation

* Corresponding author at: Materials Sciences Division, Lawrence Berkeley National Laboratory, Berkeley, CA 94720, USA. Fax: +1 510 666 3768.
*E-mail address:* vikbajaj@gmail.com (V.S. Bajaj).

1090-7807/$ - see front matter © 2011 Elsevier Inc. All rights reserved.
doi:10.1016/j.jmr.2011.06.027

of these cages with chemical targeting units, including small molecules and peptides, is now routine [6]. When xenon is dissolved into a solvent that contains sensor in sufficiently high concentration, three peaks appear in the Xe NMR spectrum: a solvent peak ($Xe_{solvent}$), at ~190 ppm in aqueous solutions, a gas peak ($Xe_{gas}$) that is conventionally referenced to 0 ppm, and a peak corresponding to xenon encapsulated in the host cage (Xe@cage). The Xe@cage frequency depends strongly on the chemical composition of the cage subunit, but is usually between 30 and 70 ppm [18]. When a xenon cage sensor binds the analyte to which it is targeted, a fourth resonance appears ($Xe@cage_{bound}$), though it may be impossible to detect without chemical exchange-based amplification. A resonance corresponding to this bound form of the sensor is a significant and differentiating feature of xenon-based molecular imaging experiments.

Most useful work with xenon-based molecular sensors is conducted at low sensor concentrations (micromolar), precluding direct detection of the Xe@cage peak. Further, many relevant bound analytes will be found in micromolar or lower concentrations, so it is generally impossible to directly detect the bound resonance. Instead, the presence of these spectroscopic species is established using indirect detection experiments that use Hyper-CEST [12]. In Hyper-CEST experiments, a saturating radiofrequency field is applied at the Xe@cage or $Xe@cage_{bound}$ frequency, causing, over time, depletion of the $Xe_{solvent}$ signal with which xenon is exchanging. The normalized intensity in the presence of saturation is a contrast parameter that is related to the concentration of the probed species.

To date, xenon-based Hyper-CEST experiments have been conducted with strong continuous wave (CW) radiofrequency fields for frequency-selective saturation. There are several limitations with this approach. First, such experiments must be designed such that the saturation field perturbs only the desired resonance and not others, a task that is complicated by the strong dependence of saturation bandwidth on the saturation power. Hyper-CEST saturation transfer is optimized for CW pulse powers that result in partial saturation of the $Xe_{solvent}$ resonance, necessitating a second reference experiment and the use of kinetic modeling for quantification of the analyte. Further, multiplexing with xenon-based molecular sensors, a technique to resolve multiple variants of the sensor simultaneously [3], relies on small frequency separations between xenon bound in slightly different host molecules, precluding the use of broad saturation pulses. A related problem involves the spatial multiplexing of arrays of xenon chemical assays on, for example, a microfluidic device; in that case, the optimum imaging approach might involve spectral–spatial selective saturation [19] or multispectral saturation pulses with Hadamard encoding [20]. Finally, the time-averaged sensitivity of these experiments depends on highly efficient saturation, but is constrained *in vivo* by limits on the specific absorption rate (SAR) of the applied pulses [21]. These constraints cannot be simultaneously satisfied in CW-based saturation experiments.

To address these concerns, we have applied band-selective saturation pulse trains in lieu of CW pulses ordinarily used in Hyper-CEST experiments. These pulses have much greater frequency selectivity than CW pulses, relaxing the conditions needed for separate control experiments. They deliver comparable saturation efficiency at much lower powers, but, depending on the choice of pulse, allow for narrow-bandwidth saturation at high pulse powers. Finally, they are compatible with slice selection and therefore with imaging sequences that depend on spatial–spectral preparation or multispectral excitation or saturation. We demonstrate the application of these saturation pulses to both spectroscopy and imaging experiments employing xenon-based molecular sensors.

## 2. Results and discussion

### 2.1. Bloch simulations of frequency-selective saturation

Preliminary to our experimental investigation of saturation transfer phenomena in solutions of xenon molecular exchange agents, we conducted Bloch equation simulations of CW and multiple pulse saturation. These simulations involved numerical solution of the Bloch equations for an exchanging spin system subject to RF irradiation of a chosen amplitude profile. The simulation took relaxation and other parameters as defined by the experimental measurements and explored parameters including pulse bandwidth, $B_1$ amplitude, saturation time, and residence time of xenon in the cryptophane-xenon complex. Because xenon binding kinetics are not known accurately from our measurements or others (though

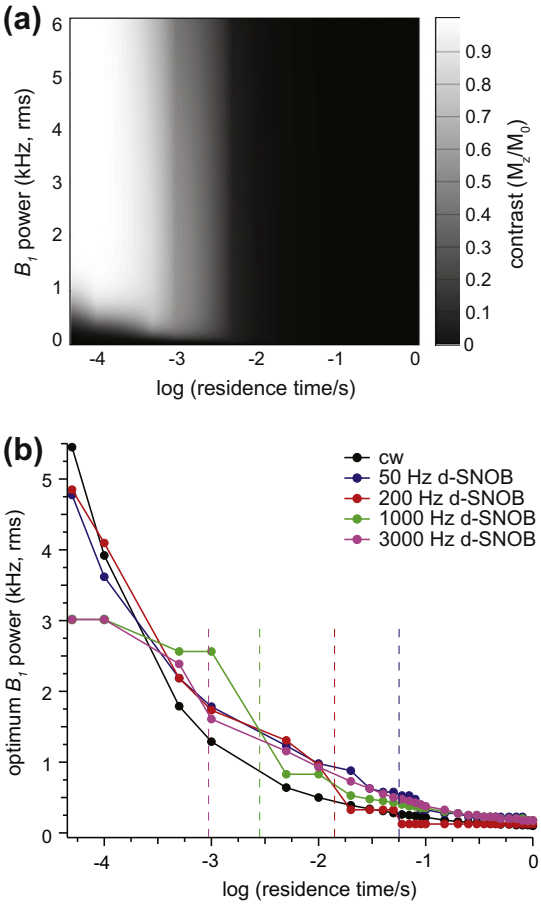


**Fig. 1.** Bloch equation simulations indicating contrast generated by various saturation parameters. (a) A contour plot illustrating the contrast generated by a CW pulse with various saturation powers, $B_1$, and on exchanging systems with difference residence times. Black indicates no contrast, while white indicates 100% contrast between an on-resonance experiment, in which the saturation is applied at the frequency of the exchanging species (Xe@cage), and an off-resonance experiment, in which the saturation is applied at a frequency equally distant from the $Xe_{aq}$ resonance, but opposite of the Xe@cage resonance. Contour plots for d-SNOB saturation pulses are visually comparable to the one shown here. (b) The best contrast is not necessarily generated by saturation pulses with the highest power; rather, the saturation pulse power for optimum contrast depends strongly on the residence time of the guest in the host. Five different saturation pulses were simulated (CW, and four d-SNOB pulses with bandwidths of 50, 200, 1000, and 3000 Hz) for a range of residence times from 50 μs to 1 s. For each pulse, the power for optimum contrast decreases with increasing residence time. While the CW pulse shows primarily exponential behavior, the d-SNOB pulses have irregular behavior, including discontinuities in the power-residence time curve. The vertical dashed lines indicate the length of time each unique d-SNOB pulse lasts. All simulation parameters are provided in Supporting Information.